Frontiers of Information Technology & Electronic Engineering
www.jzus.zju.edu.cn; engineering.cae.cn; www.springerlink.com
ISSN 2095-9184 (print); ISSN 2095-9230 (online)
E-mail: jzus@zju.edu.cn

Preparation of ultrathin ReS_2 nanosheets and their application to Q-switched Er-doped fiber lasers*

Junshan HE[1,2,3,4], Guohua ZENG[1], Shaoxian LIU[1], Haiming LU[1],
Ruixian XIE[1], Jingjing QI[1], Lili TAO[†‡1], Bo ZHOU[†‡2,3,4]

[1]*School of Materials and Energy, Guangdong University of Technology, Guangzhou 510006, China*
[2]*State Key Laboratory of Luminescent Materials and Device, South China University of Technology, Guangzhou 510641, China*
[3]*Guangdong Provincial Key Laboratory of Fiber Laser Materials and Applied Techniques, South China University of Technology, Guangzhou 510641, China*
[4]*Guangdong Engineering Technology Research and Development Center of Special Optical Fiber Materials and Devices, South China University of Technology, Guangzhou 510641, China*
[†]E-mail: taoll@gdut.edu.cn; zhoubo@scut.edu.cn

Received July 10, 2020; Revision accepted Oct. 5, 2020; Crosschecked Nov. 24, 2020

Abstract: We study the exfoliation of ultrathin ReS_2 nanosheets from the prepared ReS_2 powder and their application to Q-switched Er-doped fiber laser. XRD, Raman, and XPS spectra confirm the successful preparation of the layered ReS_2. SEM images show that the obtained ReS_2 sheets have lateral size below 200 nm. The thickness of the ReS_2 nanosheets is smaller than 5 nm according to the AFM results. ReS_2/PVA film is applied as a saturable absorber in an Er-doped Q-switched fiber laser, and a minimum pulse duration of 2.4 μs and an output power of 1.25 mW are obtained, indicating the potential application to Q-switched lasers.

Key words: Rhenium disulfide; Saturable absorber; Two-dimensional materials; Q-switched fiber laser
https://doi.org/10.1631/FITEE.2000339 **CLC number:** TN248; V254.2

1 Introduction

Optical modulation is an important area for fundamental research and has specific applications (Xing et al., 2017; Guo J et al., 2019). In recent years, two-dimensional (2D) materials, including graphene, black phosphorus (BP), transition metal dichalcogenides (TMDs), and topological insulators (TIs), have attracted significant attention due to their unique electrical, optical, and photoelectrical properties (Huang X et al., 2011; Wang QH et al., 2012; Manzeli et al., 2017; Tao et al., 2018; Zeng et al., 2018, 2019; He et al., 2019; Huang WC et al., 2020). Among them, TMDs represent a large family and include MoS_2, WS_2, $MoSe_2$, and WSe_2. The bandgaps of MoS_2, WS_2, $MoSe_2$, and WSe_2 depend greatly on the number of layers and change from direct to indirect semiconductors from monolayer to bulk layers (Tongay et al., 2012; Du J et al., 2014; Liu H et al., 2014; Wang SX et al., 2014; Zhang Y et al., 2014). As is commonly known, for most semiconducting devices, semiconductors with direct bandgaps are preferred for their better performance (Mak et al., 2010; Chen et al., 2015). Therefore, monolayer MoS_2, WS_2, $MoSe_2$, and

‡ Corresponding authors
* Project supported by the Pearl River Talent Program of Guangdong Province, China (No. 2017GC010278), the Science and Technology Program of Guangzhou, China (No. 202002030027), the National Natural Science Foundation of China (No. 61705044), and the Distinctive Innovation Project of Regular Colleges in Guangdong Province, China (No. 2018KTSCX052)
ORCID: Junshan HE, https://orcid.org/0000-0003-1705-629X; Lili TAO, https://orcid.org/0000-0002-7833-2123; Bo ZHOU, https://orcid.org/0000-0002-0701-5331

WSe_2 with large size are required for many applications, but the technology for preparing large-area monolayer TMDs is immature, thus hindering their application.

Recently, ReS_2 has attracted much attention from researchers (Qin et al., 2018; Guo ZL et al., 2019; Liu F et al., 2019; Liu Y et al., 2019). In contrast to the above mentioned TMDs, the monolayer ReS_2, few-layer ReS_2, and bulk ReS_2 are all direct semiconductors (Cui et al., 2017; Su et al., 2017). Moreover, the bandgaps of monolayer and bulk ReS_2 are 1.44 and 1.35 eV, respectively, showing a small bandgap difference (Cui et al., 2017). The physical properties of ReS_2 have little dependence on the layer number, showing a great chance of being used in practical applications.

To date, there have been several reports on Q-switched lasers based on ReS_2. For example, Su et al. (2017) reported few-layer ReS_2 as a saturable absorber (SA) for a 2.8-μm solid state laser. Lin et al. (2019) realized a 1.3-μm Q-switched solid-state laser based on a few-layer ReS_2 SA. Mao et al. (2018) reported Q-switched Er-doped fiber lasers based on ReS_2. However, almost without exception, the raw materials used are ReS_2 single crystals with high purity, which are expensive and inappropriate for large-scale applications (Mao et al., 2018; Xu et al., 2018). In this study, ReS_2 powder is first prepared using low-cost rhenium and sulfur powder as raw materials, and then ReS_2 nanosheets are obtained through liquid exfoliation of the prepared powder. ReS_2/PVA film is used as an SA in a fiber laser, showing good modulation performance for converting a continuous wave (CW) laser into a pulsed Q-switched laser. The obtained minimum pulse width is 2.4 μs, which is comparable to results realized using ReS_2 single crystals as the raw materials, indicating that the prepared ReS_2 has potential application to Er-doped Q-switched fiber lasers.

2 Experiments

ReS_2 powder was prepared in a tube furnace with an argon protective gas using rhenium and sulfur powder as raw materials. A quartz boat filled with rhenium was placed in the center of the tube furnace, while another quartz boat filled with sulfur powder was placed on the upstream side with a low temperature. The temperature of the furnace reached 750 °C in 30 min and maintained for 10 min. Then, the furnace was cooled to room temperature naturally, and thus ReS_2 powder was obtained. ReS_2 nanosheets were prepared through liquid exfoliation and centrifugal separation. In detail, 0.1 g ReS_2 powder was dispersed in a solvent, composed of the mixture of ethanol (30 mL) and deionized water (10 mL). The ReS_2 dispersion was exfoliated in an ultrasound cleaner for 12 h at a power of 400 mW. Then, the mixture was centrifuged at a speed of 5000 revolution per minute for 10 min to remove thick ReS_2. The obtained supernatant was the dispersion containing ultrathin ReS_2. Furthermore, the ReS_2 dispersion and 0.0417 g/mL PVA solution were mixed at a volume ratio of 2:3. Then, the mixture was put into an ultrasonic cleaner for 3 h and poured into an appropriate container for drying. Finally, flexible ReS_2 nanosheets/PVA film was successfully prepared.

The crystalline structure was examined by X-ray diffraction (XRD, D/MAX-Ultima IV, RigakuSmartLab, Japan) using a RigakuSmartLab X-ray diffractometer. The Raman spectra were detected using a Raman spectrometer (NOST, FEX, NOST, Korea) with a 532-nm argon ion excitation laser. X-ray photoelectron spectroscopy (XPS, Escalab 250Xi, Thermo Fisher Scientific, USA) was used to confirm the elementary composition and bonding of the prepared sample. The morphology and chemical composition were investigated using a scanning electron microscope (SEM, JSM-6490, JEOL Model, Japan) equipped with an energy dispersive spectrometer (EDS). Information on the thickness of the nanosheets was obtained through an atomic force microscopy (AFM, VeecoNanoscope V, Veeco, USA).

3 Results and discussion

Fig. 1a shows the XRD pattern of the prepared ReS_2 powder. A strong diffraction peak was detected at 2θ=14.58°, corresponding to the (001) crystal plane of ReS_2 (Jariwala et al., 2016), confirming the layer-by-layer structure along the *c*-axis. Fig. 1b presents the Raman spectra of the ReS_2 powder, nanosheets, and nanosheets/PVA film. The two low-frequency peaks located at 129.61 and 138.25 cm^{-1} are attributed to A_g modes, corresponding to the out-of-

plane vibration modes of rhenium atoms. The peaks located at 146.85, 157.18, 206.92, and 232.52 cm^{-1} are E_g modes, corresponding to the in-plane vibration modes of rhenium atoms. Other peaks located at higher frequencies come from the vibrations of lighter sulfur atoms (Feng et al., 2015; Hafeez et al., 2016). These strong vibration peaks indicate good crystallinity of the prepared ReS_2. In addition, the Raman characteristic peaks of different forms of ReS_2 do not change, except their intensity. The high-resolution XPS spectra of rhenium and sulfur are shown in Figs. 1c and 1d, respectively. The two peaks located at 41.8 and 44.2 eV correspond to $4f^{7/2}$ and $4f^{5/2}$ of rhenium, respectively. In Fig. 1d, the two peaks are fitted to be 162.25 and 163.5 eV, corresponding to $2p^{3/2}$ and $2p^{1/2}$ of sulfur, respectively. These results strongly agree with other reported XPS spectra of ReS_2, confirming the successful preparation of ReS_2 (Hafeez et al., 2016).

Figs. 2a–2c are the SEM images obtained at different magnifications, showing that the prepared ReS_2 are thin nanosheets with lateral size below 200 nm. Fig. 2d shows the EDX spectrum of the sample, confirming that the component elements are rhenium and sulfur, and that the ratio of Re:S is 0.5731:1, which is close to the ratio of Re:S in ReS_2. To determine the thickness of the ReS_2 nanosheets, AFM characterization was carried out (Figs. 2e and 2f). The AFM image (Fig. 2e) indicates that the ReS_2 sheets are nanosized and ultrathin. The height profiles of some randomly selected ReS_2 nanosheets are given in Fig. 2f, showing that all the thicknesses of the nanosheets are below 5 nm. As the interlayer spacing of the few-layer ReS_2 is 0.7 nm (Liu EF et al., 2016), the number of layers of the prepared ReS_2 nanosheets is estimated to be less than 7.

Fig. 3 shows the experimental setup of the Q-switched Er-doped fiber laser based on the ReS_2

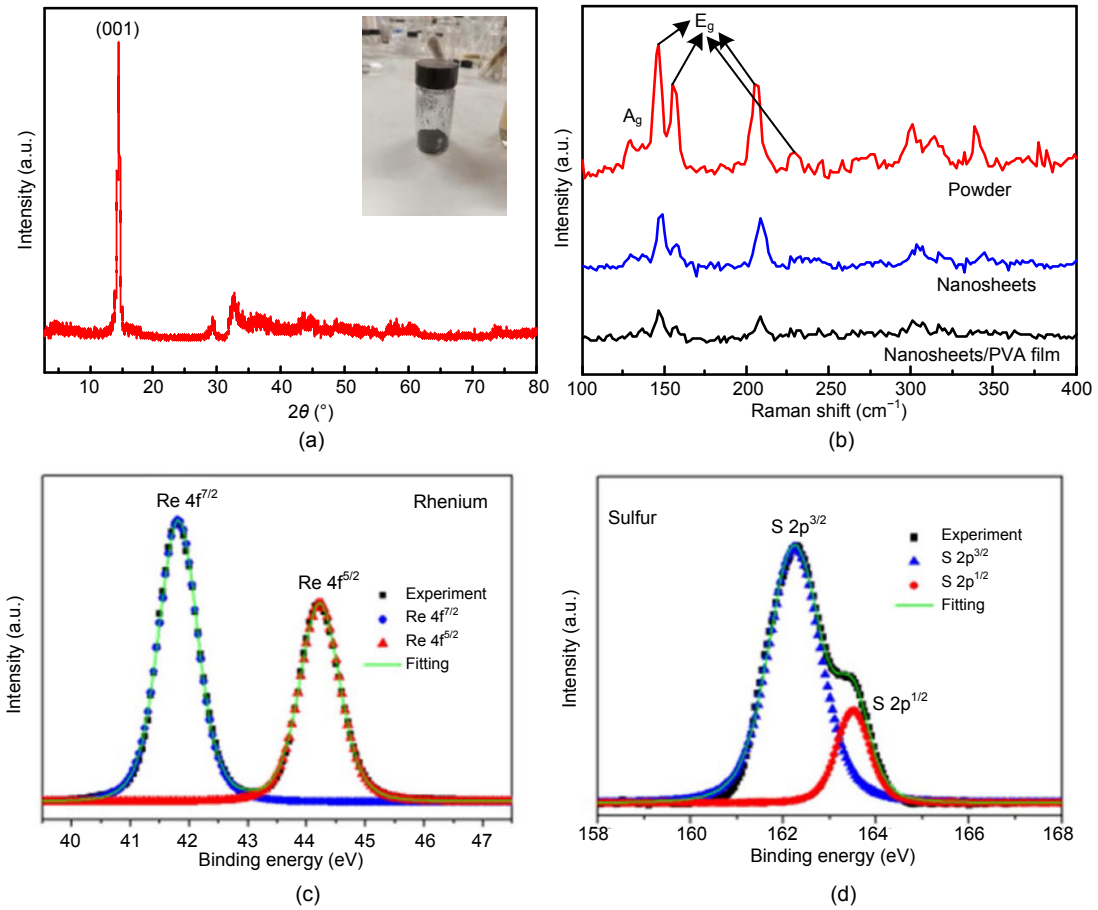

Fig. 1 (a) XRD pattern of the prepared ReS_2 powder (inset is a photograph of the powder); (b) Raman spectra of the ReS_2 powder, nanosheets, and nanosheets/PVA film; (c) high resolution XPS spectra of Re 4f; (d) high resolution XPS spectra of S 2p

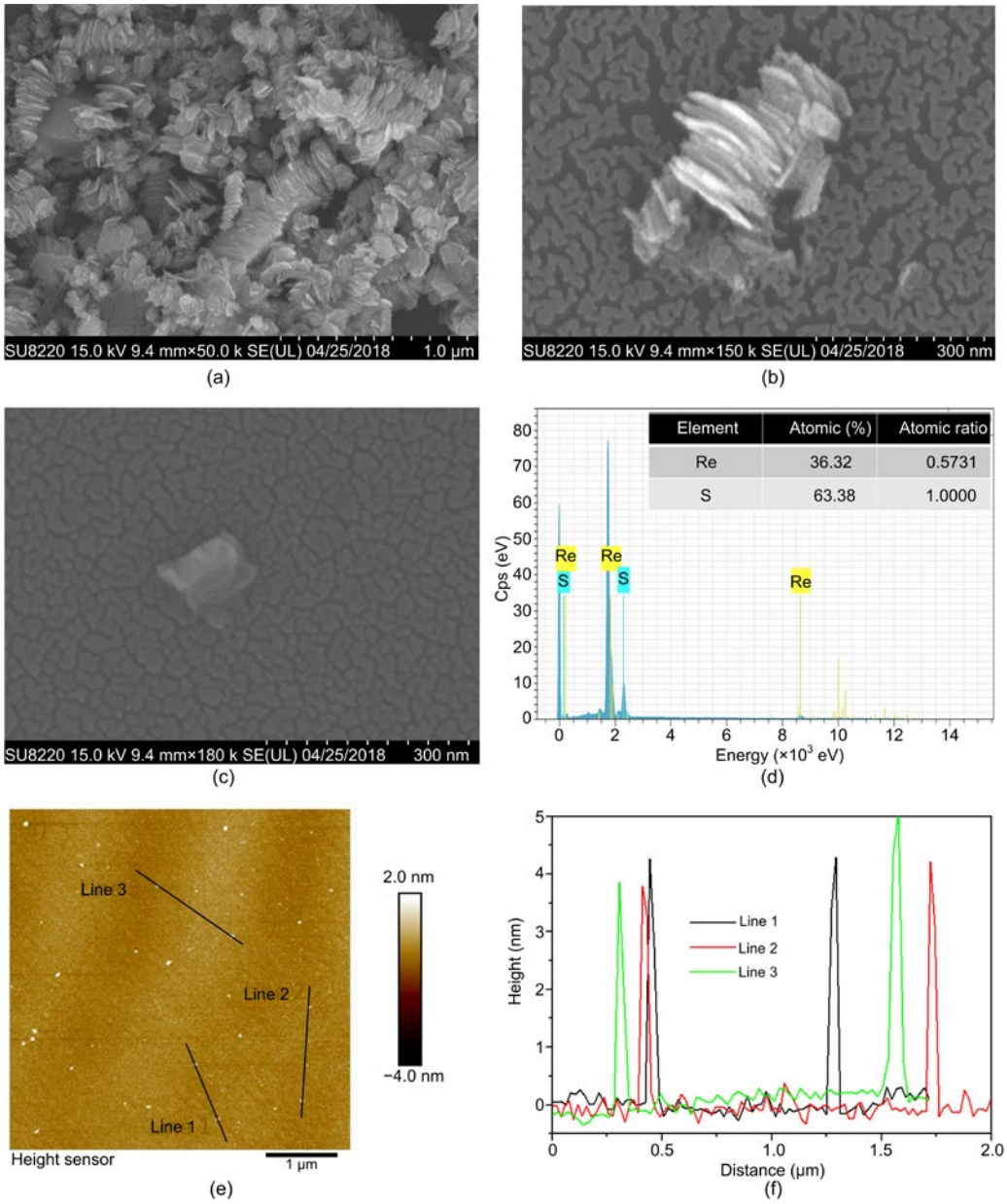

Fig. 2 (a–c) SEM images; (d) EDX spectrum; (e) AFM image; (f) height profile of the ReS_2 nanosheets marked in (e) (References to color refer to the online version of this figure)

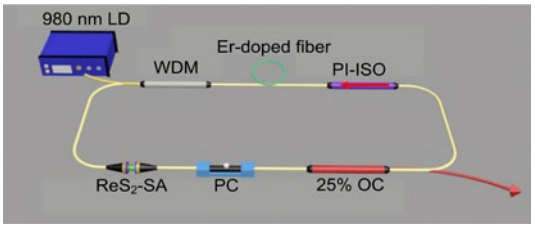

Fig. 3 Experimental setup of the Q-switched Er-doped fiber laser based on ReS_2 saturable absorber (SA)

LD: laser diode; WDM: wavelength division multiplexer; PI-ISO: polarization-independent isolator; PC: polarization controller; OC: output coupler

SA. A laser diode (LD) centered at the wavelength of 976 nm with the maximum power of 500 mW was used as the pump source. The pump energy was delivered into a piece of 2 m-long Er-doped fiber via a 980/1064 wavelength division multiplexer (WDM). A polarization-independent isolator (PI-ISO) was connected to ensure the unidirectional signal propagation in the cavity. A 75:25 output coupler (OC) was used to extract the output signal. The total length of the cavity was 8.4 m.

In this experiment, we first inserted a pure PVA film into the laser cavity and increased the pump power. Even when the pump power was up to 400 mW or the PC was constantly adjusted, the laser worked only in a CW mode. Then, the ReS_2/PVA film was inserted into the laser cavity, and a Q-switching signal was obtained when the pump power was increased to about 120 mW. Fig. 4a shows the pulse trains with a pulse duration of 2.8 μs of the Q-switched Er-doped fiber laser based on ReS_2 SA obtained at a pump power of 160 mW. Fig. 4b demonstrates the evolution of the repetition rate and pulse duration with an increasing pump power. The repetition rate became higher, from 56.8 to 66.52 kHz, and the pulse duration narrowed from 9.74 to 2.4 μs with an increasing pump power, showing the typical characteristics of a Q-switched laser. Fig. 4c shows the average output power and single pulse energy vs. pump power. The maximum output power and single pulse energy were 1.25 mW and 18.88 nJ, respectively. Performance comparison of Q-switched Er-doped fiber lasers based on different TMDs is summarized in Table 1, indicating that the performance of the Q-switched Er-doped fiber laser based

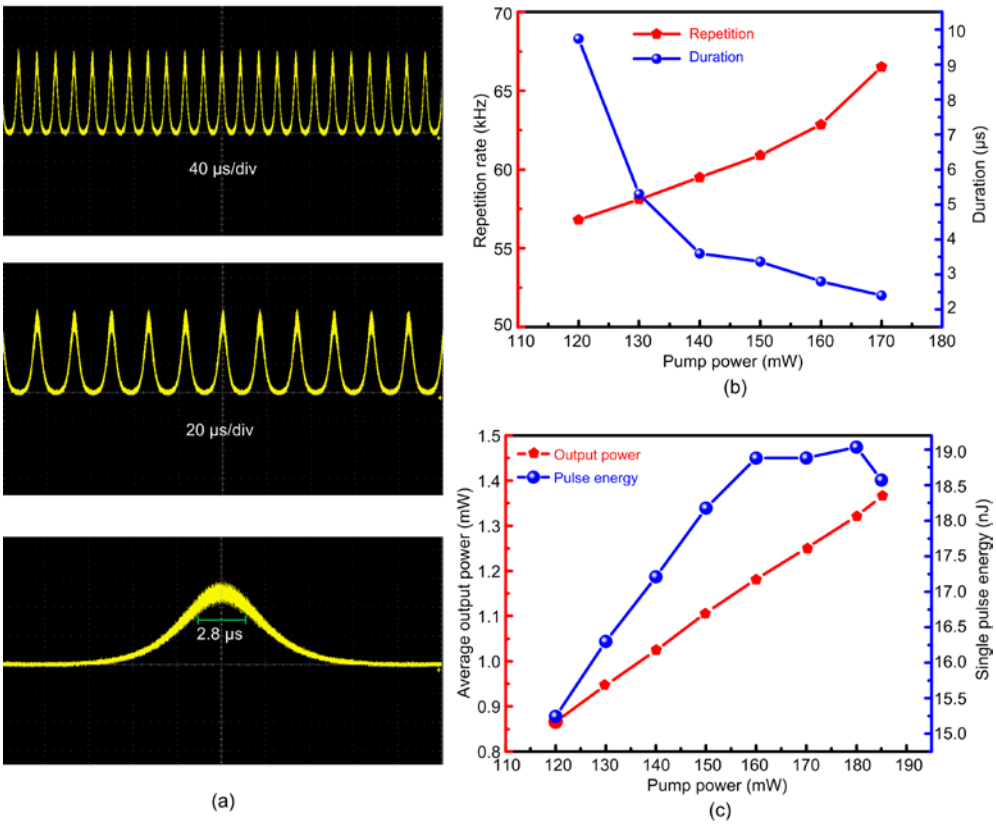

Fig. 4 (a) Q-switched pulse trains in different scales obtained at a pump power of 160 mW; (b) repetition rate and pulse duration vs. pump power; (c) average output power and single pulse energy vs. pump power

Table 1 Performance comparison of Q-switched Er-doped fiber lasers based on different TMDs

Material	Pulse duration (μs)	Maximum output power (mW)	Repetition rate (kHz)	Maximum pulse energy (nJ)	Reference
MoS_2	23.3–5.4	1.70	6.5–27	63.20	Luo et al. (2014)
WS_2	3.4–1.1	16.40	79–97	179.60	Zhang M et al. (2015)
$ReSe_2$	16.5–4.98	0.76	6.64–21.04	36.00	Du L et al. (2018)
$PtSe_2$	4.6–0.9	11.34	20.5–79.2	143.20	Zhang K et al. (2018)
PtS_2	9.6–4.2	1.10	18.1–24.6	45.60	Wang XY et al. (2018)
ReS_2	7.4–2.1	2.48	43–64	38.00	Xu et al. (2018)
ReS_2	23–5.496	1.20	12.6–19	62.80	Mao et al. (2018)
ReS_2	9.74–2.4	1.25	56.8–66.52	18.88	This work

on ReS_2 in this research is comparable to those of other reported ones. However, it is noteworthy that the ReS_2 nanosheets prepared in this work were exfoliated from low-cost powder, while the raw material used in other work was ReS_2 single crystal, purchased at high expenses.

4 Conclusions

We have studied a Q-switched Er-doped fiber laser based on ultrathin ReS_2 nanosheets exfoliated from the prepared low-cost ReS_2 powder. XRD pattern, Raman spectrum, XPS spectra, and EDX results indicated the successful preparation of ReS_2. The thickness of the ReS_2 nanosheets was below 5 nm according to the AFM results. The realized Q-switched Er-doped fiber laser based on ReS_2 had a minimum pulse duration of 2.4 μs with a repetition of 66.52 kHz, indicating that the prepared ultrathin ReS_2 nanosheets have potential application as saturable absorbers to Q-switched fiber lasers.

Contributors

Lili TAO and Bo ZHOU designed the research. Junshan HE, Guohua ZENG, Shaoxian LIU, and Haiming LU conducted the experiments and processed the data. Junshan HE drafted the manuscript. Ruixian XIE and Jingjing QI helped organize the manuscript. Lili TAO and Bo ZHOU revised and finalized the paper.

Compliance with ethics guidelines

Junshan HE, Guohua ZENG, Shaoxian LIU, Haiming LU, Ruixian XIE, Jingjing QI, Lili TAO, and Bo ZHOU declare that they have no conflict of interest.

References

Chen BH, Zhang XY, Wu K, et al., 2015. Q-switched fiber laser based on transition metal dichalcogenides MoS_2, $MoSe_2$, WS_2, and WSe_2. *Opt Expr*, 23(20):26723-26737. https://doi.org/10.1364/OE.23.026723

Cui YD, Lu FF, Liu XM, 2017. Nonlinear saturable and polarization-induced absorption of rhenium disulfide. *Sci Rep*, 7:40080. https://doi.org/10.1038/srep40080

Du J, Wang QK, Jiang GB, et al., 2014. Ytterbium-doped fiber laser passively mode locked by few-layer molybdenum disulfide (MoS_2) saturable absorber functioned with evanescent field interaction. *Sci Rep*, 4:6346. https://doi.org/10.1038/srep06346

Du L, Jiang GB, Miao LL, et al., 2018. Few-layer rhenium diselenide: an ambient-stable nonlinear optical modulator. *Opt Mater Expr*, 8(4):926-935. https://doi.org/10.1364/OME.8.000926

Feng YQ, Zhou W, Wang YJ, et al., 2015. Raman vibrational spectra of bulk to monolayer ReS_2 with lower symmetry. *Phys Rev B*, 92(5):054110. https://doi.org/10.1103/PhysRevB.92.054110

Guo J, Zhao JL, Hunag DZ, et al., 2019. Two-dimensional tellurium-polymer membrane for ultrafast photonics. *Nanoscale*, 11(13):6235-6242. https://doi.org/10.1039/C9NR00736A

Guo ZL, Wei AX, Zhao Y, et al., 2019. Controllable growth of large-area atomically thin ReS_2 films and their thickness-dependent optoelectronic properties. *Appl Phys Lett*, 114(15):153102. https://doi.org/10.1063/1.5087456

Hafeez M, Gan L, Li HQ, et al., 2016. Large-area bilayer ReS_2 film/multilayer ReS_2 flakes synthesized by chemical vapor deposition for high performance photodetectors. *Adv Funct Mater*, 26(25):4551-4560. https://doi.org/10.1002/adfm.201601019

He JS, Tao LL, Zhang H, et al., 2019. Emerging 2D materials beyond graphene for ultrashort pulse generation in fiber lasers. *Nanoscale*, 11(6):2577-2593. https://doi.org/10.1039/C8NR09368G

Huang WC, Li C, Gao LF, et al., 2020. Emerging black phosphorus analogue nanomaterials for high-performance device applications. *J Mater Chem C*, 8(4):1172-1197. https://doi.org/10.1039/c9tc05558d

Huang X, Yin ZY, Wu SX, et al., 2011. Graphene-based materials: synthesis, characterization, properties, and applications. *Small*, 7(14):1876-1902. https://doi.org/10.1002/smll.201002009

Jariwala D, Voiry D, Jindal A, et al., 2016. Synthesis and characterization of ReS_2 and $ReSe_2$ layered chalcogenide single crystals. *Chem Mater*, 28(10):3352-3359. https://doi.org/10.1021/acs.chemmater.6b00364

Lin MX, Peng QQ, Hou W, et al., 2019. 1.3 μm Q-switched solid-state laser based on few-layer ReS_2 saturable absorber. *Opt Laser Technol*, 109:90-93. https://doi.org/10.1016/j.optlastec.2018.07.062

Liu EF, Long MS, Zeng JW, et al., 2016. High responsivity phototransistors based on few-layer ReS_2 for weak signal detection. *Adv Funct Mater*, 26(12):1938-1944. https://doi.org/10.1002/adfm.201504408

Liu F, Zhao X, Yan XQ, et al., 2019. Ultrafast nonlinear absorption and carrier relaxation in ReS_2 and $ReSe_2$ films. *J Appl Phys*, 125(17):173105. https://doi.org/10.1063/1.5093757

Liu H, Luo AP, Wang FZ, et al., 2014. Femtosecond pulse erbium-doped fiber laser by a few-layer MoS_2 saturable absorber. *Opt Lett*, 39(15):4591-4594. https://doi.org/10.1364/OL.39.004591

Liu Y, An QW, Meng XQ, 2019. Controllable growth of vertical ReS_2 nanosheets and nanorods by vapor transport method. *J Mater Sci*, 54(9):6807-6814. https://doi.org/10.1007/s10853-019-03395-x

Luo ZQ, Huang YZ, Zhong M, et al., 2014. 1-, 1.5-, and 2-μm fiber lasers Q-switched by a broadband few-layer MoS_2

saturable absorber. *J Lightw Technol*, 32(24):4679-4686. https://doi.org/10.1109/jlt.2014.2362147

Mak KF, Lee C, Hone J, et al., 2010. Atomically thin MoS_2: a new direct-gap semiconductor. *Phys Rev Lett*, 105(13): 136805. https://doi.org/10.1103/PhysRevLett.105.136805

Manzeli S, Ovchinnikov D, Pasquier D, et al., 2017. 2D transition metal dichalcogenides. *Nat Rev Mater*, 2(8):17033. https://doi.org/10.1038/natrevmats.2017.33

Mao D, Cui XQ, Gan XT, et al., 2018. Passively Q-switched and mode-locked fiber laser based on an ReS_2 saturable absorber. *IEEE J Sel Top Quant Electron*, 24(3):1100406. https://doi.org/10.1109/JSTQE.2017.2713641

Qin JK, Qiu G, He W, et al., 2018. Epitaxial growth of 1D atomic chain based Se nanoplates on monolayer ReS_2 for high-performance photodetectors. *Adv Funct Mater*, 28(48):1806254. https://doi.org/10.1002/adfm.201806254

Su XC, Nie HK, Wang YR, et al., 2017. Few-layered ReS_2 as saturable absorber for 2.8 μm solid state laser. *Opt Lett*, 42(17):3502-3505. https://doi.org/10.1364/OL.42.003502

Tao LL, Huang XW, He JS, et al., 2018. Vertically standing $PtSe_2$ film: a saturable absorber for a passively mode-locked Nd:$LuVO_4$ laser. *Photon Res*, 6(7):750-755. https://doi.org/10.1364/PRJ.6.000750

Tongay S, Zhou J, Ataca C, et al., 2012. Thermally driven crossover from indirect toward direct bandgap in 2D semiconductors: $MoSe_2$ versus MoS_2. *Nano Lett*, 12(11): 5576-5580. https://doi.org/10.1021/nl302584w

Wang QH, Kalantar-Zadeh K, Kis A, et al., 2012. Electronics and optoelectronics of two-dimensional transition metal dichalcogenides. *Nat Nanotechnol*, 7(11):699-712. https://doi.org/10.1038/NNANO.2012.193

Wang SX, Yu HH, Zhang HJ, et al., 2014. Broadband few-layer MoS_2 saturable absorbers. *Adv Mater*, 26(21):3538-3544. https://doi.org/10.1002/adma.201306322

Wang XY, Cheng PK, Tang CY, et al., 2018. Laser Q-switching with PtS_2 microflakes saturable absorber. *Opt Express*, 26(10):13055-13060. https://doi.org/10.1364/OE.26.013055

Xing CY, Xie ZJ, Liang ZM, et al., 2017. 2D nonlayered selenium nanosheets: facile synthesis, photoluminescence, and ultrafast photonics. *Adv Opt Mater*, 5(24):1700884. https://doi.org/10.1002/adom.201700884

Xu X, Jiang M, Li D, et al., 2018. Passive Q-switching based on ReS_2 saturable absorber in Er-doped fiber laser at 1532 nm. *Opt Quant Electron*, 50(1):39. https://doi.org/10.1007/s11082-017-1281-3

Zeng LH, Lin SH, Li ZJ, et al., 2018. Fast, self-driven, air-stable, and broadband photodetector based on vertically aligned $PtSe_2$/GaAs heterojunction. *Adv Funct Mater*, 28(16):1705970. https://doi.org/10.1002/adfm.201705970

Zeng LH, Wu D, Lin SH, et al., 2019. Controlled synthesis of 2D palladium diselenide for sensitive photodetector applications. *Adv Funct Mater*, 29(1):1806878. https://doi.org/10.1002/adfm.201806878

Zhang K, Feng M, Ren YY, et al., 2018. Q-switched and mode-locked Er-doped fiber laser using $PtSe_2$ as a saturable absorber. *Photon Res*, 6(9):893-899. https://doi.org/10.1364/PRJ.6.000893

Zhang M, Hu GH, Hu GQ, et al., 2015. Yb- and Er-doped fiber laser Q-switched with an optically uniform, broadband WS_2 saturable absorber. *Sci Rep*, 5:17482. https://doi.org/10.1038/srep17482

Zhang Y, Chang TR, Zhou B, et al., 2014. Direct observation of the transition from indirect to direct bandgap in atomically thin epitaxial $MoSe_2$. *Nat Nanotechnol*, 9(2):111-115. https://doi.org/10.1038/NNANO.2013.277